Supporting Information

for

Effect of Acid Treatment on Activated Carbon: Preferential Attachment and Stronger Binding of Metal Nanoparticles on External Carbon Surface, with Higher Metal Ion Release, for Superior Water Disinfection

Pritam Biswas and Rajdip Bandyopadhyaya*

Department of Chemical Engineering, Indian Institute of Technology Bombay,

Powai, Mumbai 400076, India.

* Corresponding author:

 E-mail: rajdip@che.iitb.ac.in

 Tel: +91 (22) 2576 7209   Fax: +91 (22) 2572 6895

A.1 Batch mode cell-death experiments with Ag-p-AC and Ag-a-AC using *E. coli*

Ag-a-AC granule was sieved with a 20×40 mesh sieve and further used of batch mode cell-death experiments. For checking the cell-death performance of the granule, *Escherichia coli* K12 (MTCC 1302, Chandigarh, India) was selected a model organism. Cells were grown in Luria bertani (LB) (Merck, India) to have a cell concentration of 10^8 CFU/ml. Subsequently, the cells were washed and resuspended in PBS buffer [sodium chloride (NaCl), potassium chloride (KCl), disodium phosphate (Na_2HPO_4), potassium dihydrogen phosphate (KH_2PO_4) (Merck, India)] having a final concentration of 10^4 CFU/ml. Typically, 800 mg of Ag-p-AC granules were added to 100 ml of cell suspension (i.e. 8 mg of granules/ml of cell suspension) and incubated at 37º C at a mixing speed of 150 rpm. After every, 5 min of time interval samples were collected and plated in the agar plate. The cell concentration was also measured for different concentrations (2, 4, 6 and 8 mg/ml) using Ag-a-AC.

The time dependent cell count has also been measured by fluorescence spectroscopy. After collection of cell samples, two fluorescence dyes, namely, 4', 6-diamidino-2-phenylindole (DAPI) and propidium iodide (PI) (Invitrogen, Life Technologies, India) were added. The concentrations of both the dyes were optimized to ensure staining of all the cells (Figure S2, Supporting Information). For all the samples, the fluorescence intensity was measured for both the dyes. The cell concentration was calculated based on the calibration plot (Figure S3, Supporting Information).

In batch mode using 8 mg/ml of Ag-p-AC (shown as a representative plot for minimal contact time or residence time requirement)[1] and Ag-a-AC, zero live cell concentration was achieved in 25 and 15 min, (from 10^4 CFU/ml) of residence time [Figure S1a], respectively. Experiments were also performed for 2,4 and 6 mg/ ml of both the hybrid. As before, experiments were performed using 2,

4 and 6 mg/ml of Ag-a-AC hybrid. In all the cases the fluorescence spectroscopy data shows a good match with the plate count data.
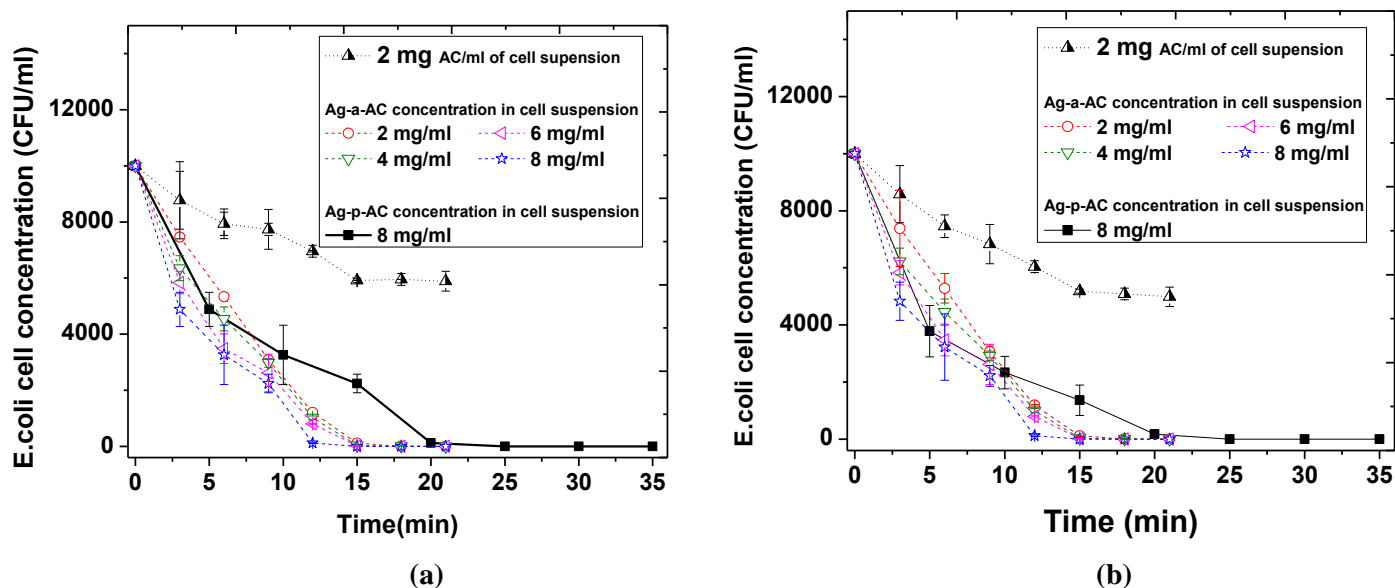

Figure S1. (a) Measurement of *E. coli* cell concentration by plate count method during batch mode shake flask experiments, using an initial cell concentration of 10^4 CFU/ml, for different concentration of hybrids (2, 4, 6 and 8 mg/ml of cell suspension) using Ag-a-AC hybrid and a representative data was also shown for 8 mg/ml of Ag-p-AC with minimal residence time requirement. (b) Cell-concentrations were also quantified by fluorescence spectroscopy for all the Ag-a-AC samples with different concentration and 8 mg/ml of Ag-p-AC.

A.2 Fluorescence microscopy imaging of *E. coli* cells

A single live *E. coli* cell was imaged in a cryo-SEM. Phase contrast image shows a population of *E. coli* cells [Figure S2b]. As cells were smaller in size (beyond a normal microscope's range), visibility of cells were not very good in this image. 4', 6-diamidino-2-phenylindole (DAPI) and propidium iodide (PI) have been used as fluorescence dyes for quantifying the live and dead *E. coli*
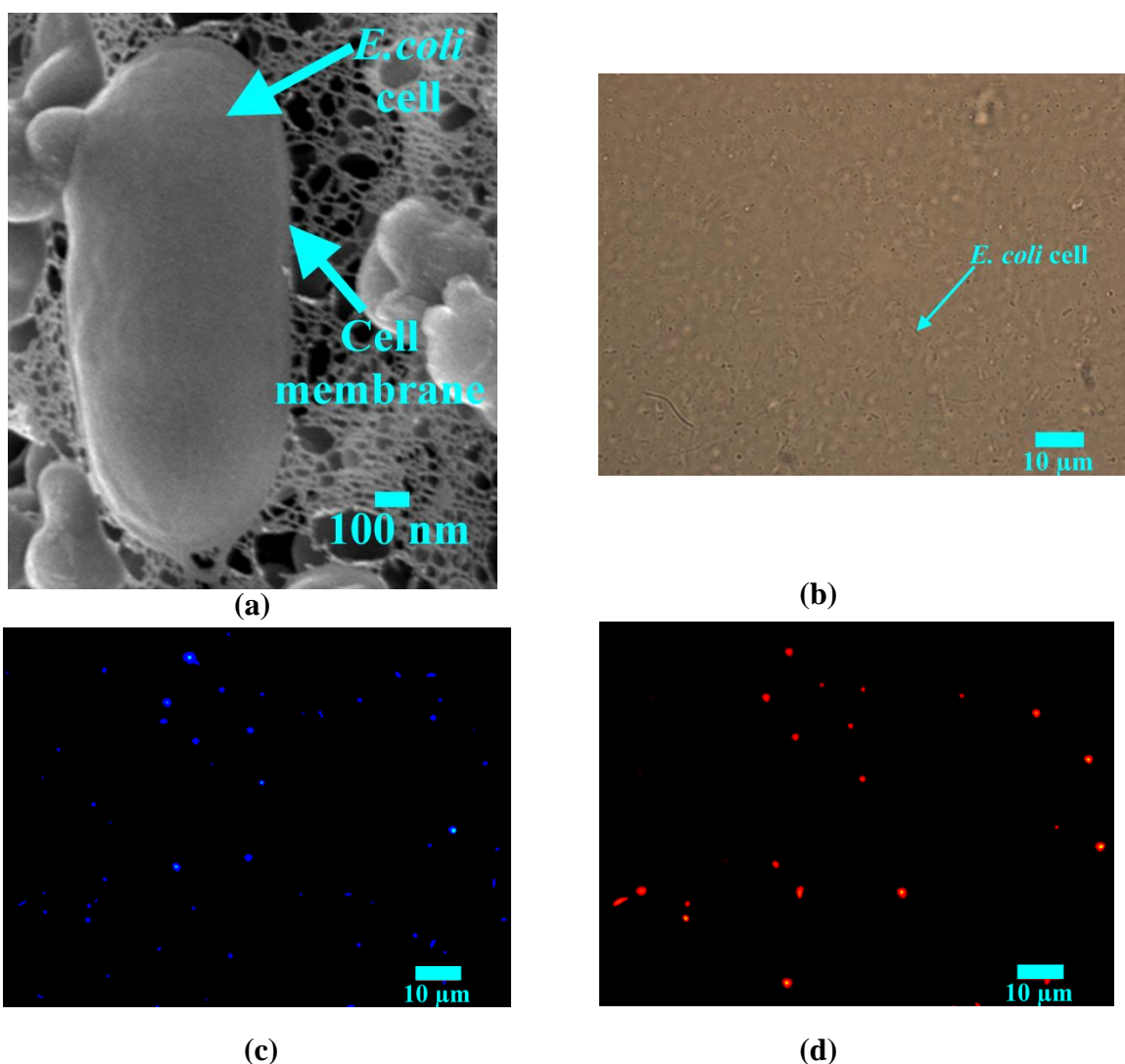
3

Figure S2. (a) Cryo-SEM image of a single *E. coli* cell. Images (b-d) of a population of cells: (b) Phase contrast image under microscope (c) Fluorescence microscopy image of DAPI stained live and dead cells and (d) PI stained dead cells.

cells. The dye concentration was optimized to ensure that all the cells were stained and then the cells were viewed in a fluorescence microscope. Three different cell samples were prepared and imaged in the fluorescence microscope, namely, (a) only live cells (b) only dead cell and (c) mixture of live and dead cells. DAPI stains all the cells (live and dead both). PI stains only dead cells. It was ensured from the phase contrast and fluorescence microscopy images that for all three samples, all cells were

4

stained (for live and dead cells stained with DAPI and dead cell stained with PI). Therefore, the working concentration range was optimized and used for further quantitative measurements.

A.3 Calibration plots from fluorescence spectroscopy measurements

Known number of only live and only dead cell suspension was prepared in PBS buffer. DAPI and PI were added in both the samples in excess amount (as optimized earlier). Further the cells were washed multiple times with PBS buffer for removing excess dye and the fluorescence intensity was measured using a fluorescence spectrometer. Calibration plots were generated for DAPI and PI as shown above [Figure S3]. This calibration plot was already mentioned in Biswas and Bandyopadhyaya's (2016)[1] supplementary information.
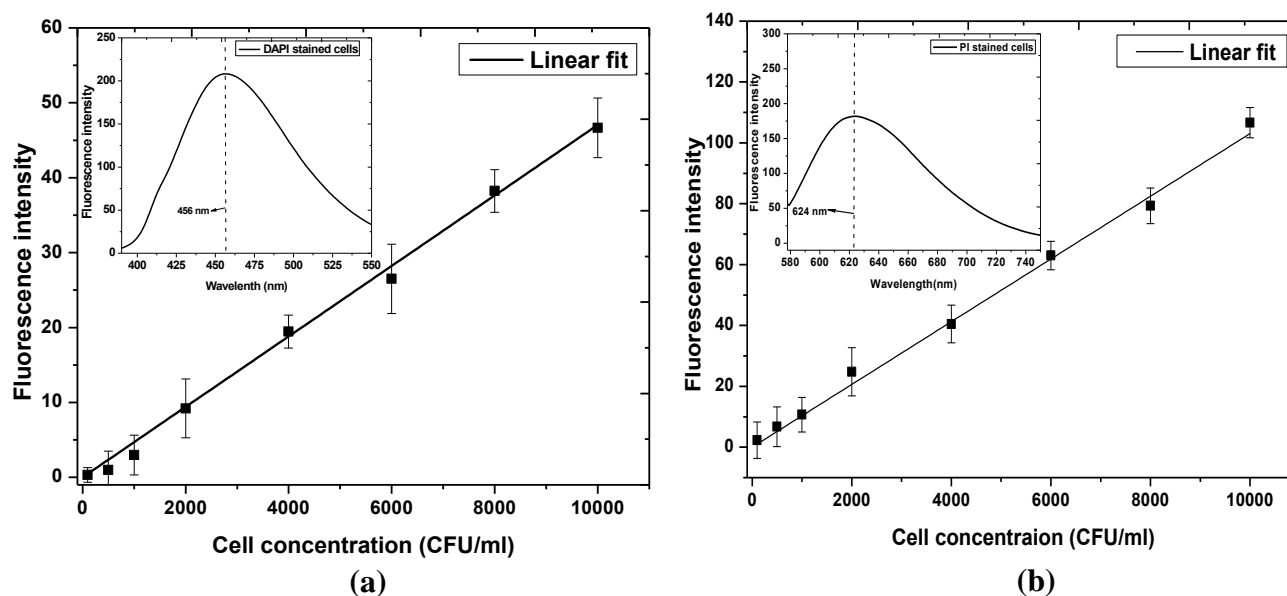
Figure S3. Calibration plot for calculating (a) total (live and dead) cell count using DAPI and (b) dead cell count using PI. Error bars were added from three independent experiments, measuring 2 samples from each experiment. Inset plot shows fluorescence intensity plots for DAPI and PI attached *E. coli* cells.

A.4 Batch mode cell-death experiments with Ag-p-AC and Ag-a-AC using *B.subtilis*

Figure S4 shows the required contact time to completely kill 10^4 CFU/ml of *Bacillus subtilis* 168 using different concentrations of Ag-p-AC and Ag-a-AC hybrid, respectively. Using 8 mg/ml of Ag-a-AC, 4 log reduction in cell concentration is achieved in only 3 min, which is significantly less compared to the same 8 mg/ml concentration of Ag-p-AC, which needed 10 min. Therefore, Ag-a-AC also displays faster cell-death for a gram positive bacteria *Bacillus subtilis,* as for *E. coli* too. This confirms the generality of our hybrid in ensuring complete destruction of both gram-positive and gram-negative microorganisms.
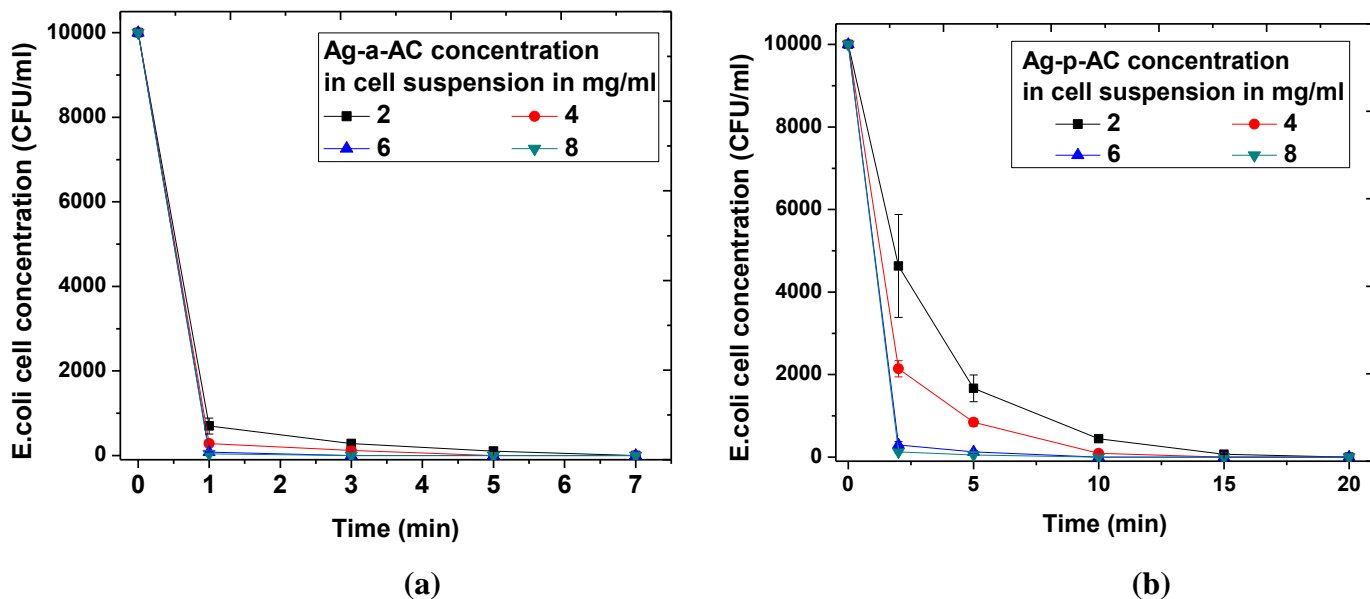

Figure S4. (a) Measurement of *B. subtilis* cell concentration by plate count method during batch mode shake flask experiments, using an initial cell concentration of 10^4 CFU/ml, for different concentration of hybrids (2, 4, 6 and 8 mg/ml of cell suspension) using (a) Ag-a-AC and (b) Ag-p-AC.

A.5 FEG-SEM images of Ag-un-AC hybrid showing complete and partial pore blockage due to Ag-NP attachment

FEG-SEM images of Ag-un-AC hybrid with different magnification and pore diameter to show complete and partial pore blockage due to attachment of Ag-NPs. Figure S5a shows
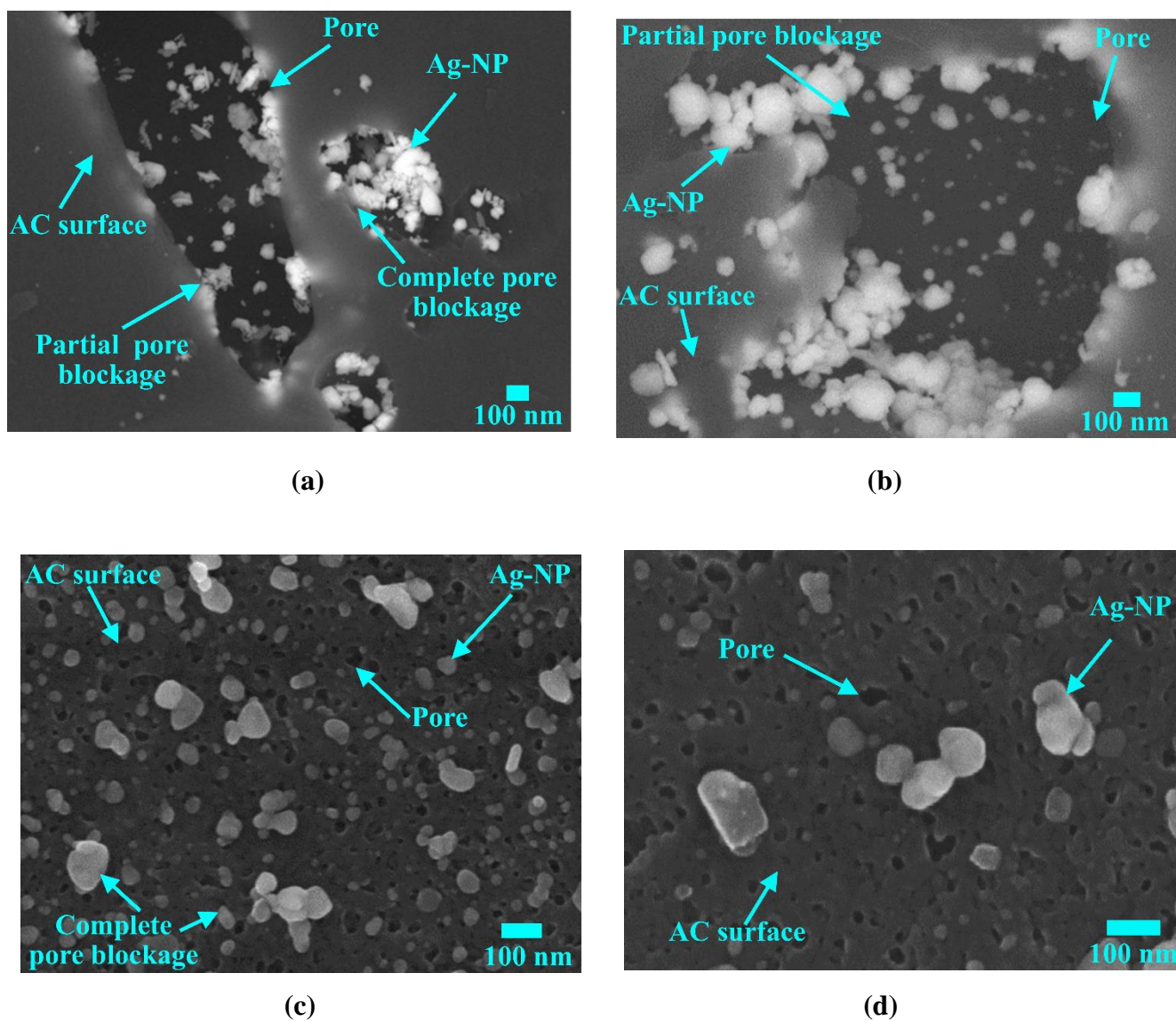

(a)

(b)

(c)

(d)

Figure S5. FEG-SEM images of Ag-un-AC granules with different magnification showing pores with Ag-NPs attached on un-AC. Figure (a) shows partial or complete pore blockage due to attachment of

Ag-NPs inside the pores of un-AC. Fig. (b) shows magnified image of partial pore blockage due to attachment of Ag-NPs on the pore mouth as well as pore interiors. Fig. (c) shows complete pore blockage due to attachment of comparatively (with respect to the pore size) larger Ag-NP. Fig. (d) shows attachment of Ag-NPs on the pore mouth resulting complete pore blockage.

FEG-SEM images of micron size pores either partially or completely blocked with Ag-NPs, for Ag-un-AC hybrid. Figure S5b shows magnified view of partially blocked pore. For pores with a diameter in the range of nanometers, some of the pores were partially blocked due to attachment of Ag-NPs on the pore mouth and some of the pore are completely blocked as the pore size is smaller the NP size [Figures S5 c and d below].

As a cumulative effect of these complete pore blockage and partial pore blockage a significant decrease in pore volume (59.5% decrease in pore volume after Ag-NP impregnation on Ag-un-AC) is observed in the porosimetry measurement.

A.6 FEG-SEM images of Ag-un-AC, Ag-p-AC and Ag-a-AC with lower magnification

For better clarity in understanding the location of Ag-NP attachment on different AC samples, images of Ag-un-AC [in Figure S6a-b], Ag-p-AC [in Figures S6c-d] and Ag-a-AC [in Figure S6e-f] hybrid were shown below. It is clear from Figures S6a and b that, for untreated AC, most of the Ag-NPs are present on the pore mouth or pore interior, while most of the external surface of AC has very less Ag-NPs. Hence, most of the Ag-NPs remain inaccessible to the *E. coli* cells in the subsequent cell-killing experiment. In contrast, for Ag-p-AC and Ag-a-AC, most of the Ag-NPs are
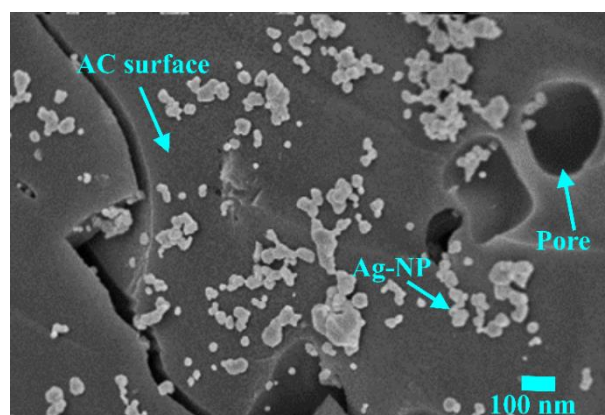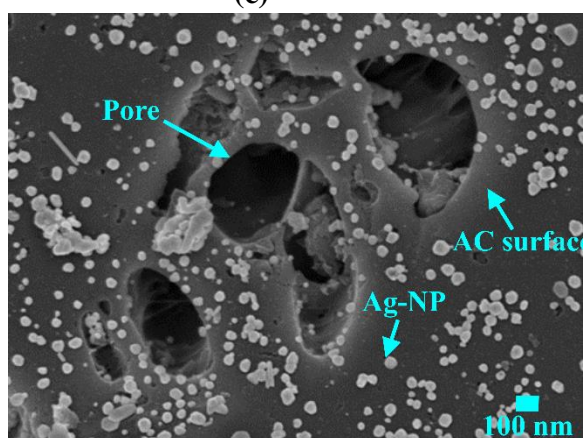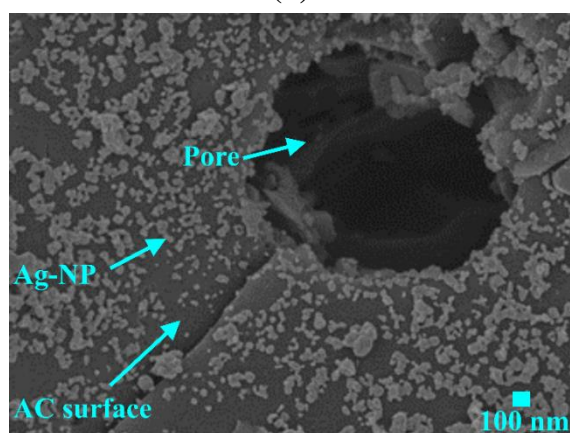
8
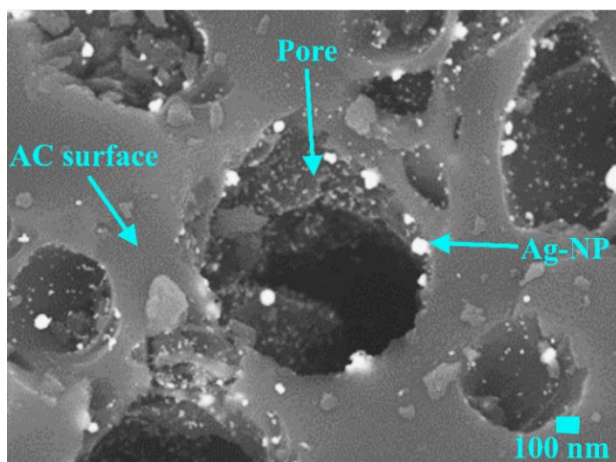
(a)
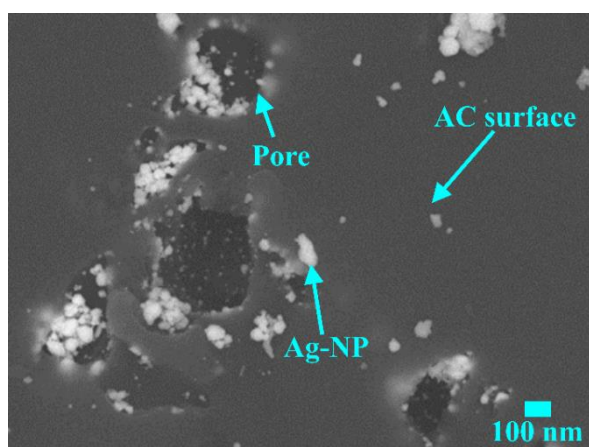
(b)
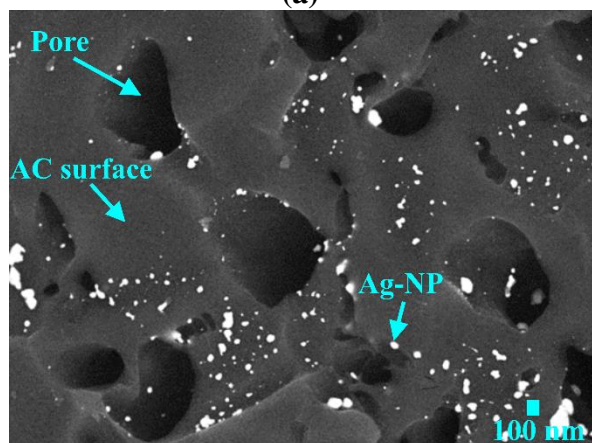
(c)

(d)

(e)

(f)

Figure S6. FEG-SEM images of (a, b) Ag-un-AC, (c,d) Ag-p-AC and (e,f) Ag-a-AC hybrid. Figure a and b shows attachment of Ag-NPs mostly on the pore interior. Figures c-f shows attachment of Ag-NPs mostly on the external surface.

present on the external surface of AC, instead of pore interiors [Figures S6c-f], ensuring good contact between the *E. coli* cell and the Ag-NPs. Therefore, Ag-a-AC has higher amount of Ag-NPs on the external surface of AC. Therefore, a higher cell-killing efficiency was observed during water disinfection.

A.7 Contact angle measurement using a water drop

For measuring the wettability of the AC surface after plasma and acid treatment the contact angle was measured for after placing a water drop in a goniometer. In case of untreated AC, the average contact angle was 112° based on six measurements [Figure S7 a]. For both
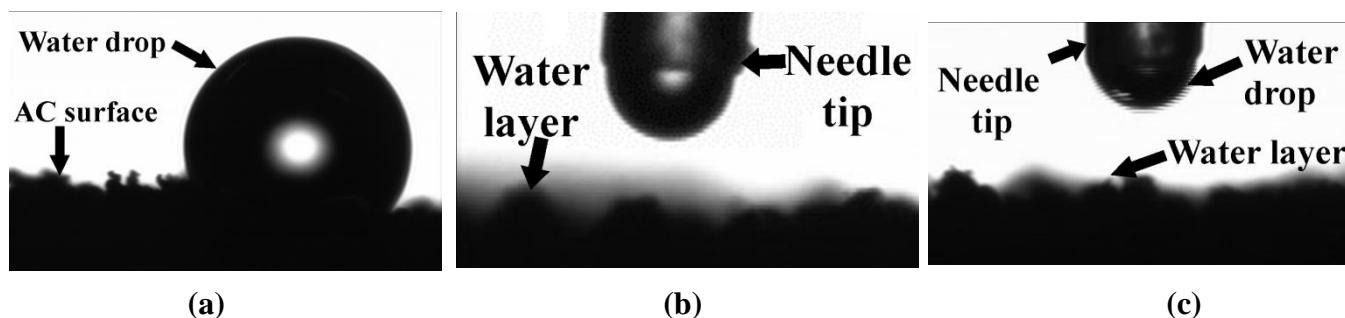

(a)   (b)   (c)

Figure S7. Quantification of contact angle using a water drop on the external surface of (a) untreated AC, (b) plasma treated AC and (c) acid treated AC.

plasma and acid treated AC samples the water drop penetrates inside the surface almost instantaneously and forms a thin layer of water, confirming the increase in hydrophilicity of the AC [Figure S7b and c]. This is favorable for our application as better wetting will also ensure better contact between AC surface and *E. coli* cells.

A.8 Elemental mapping of un-AC, Ag-p-AC and Ag-a-AC

(a) Carbon **(b)** Silver **(c)**

(d) Carbon **(e)** Silver **(f)**
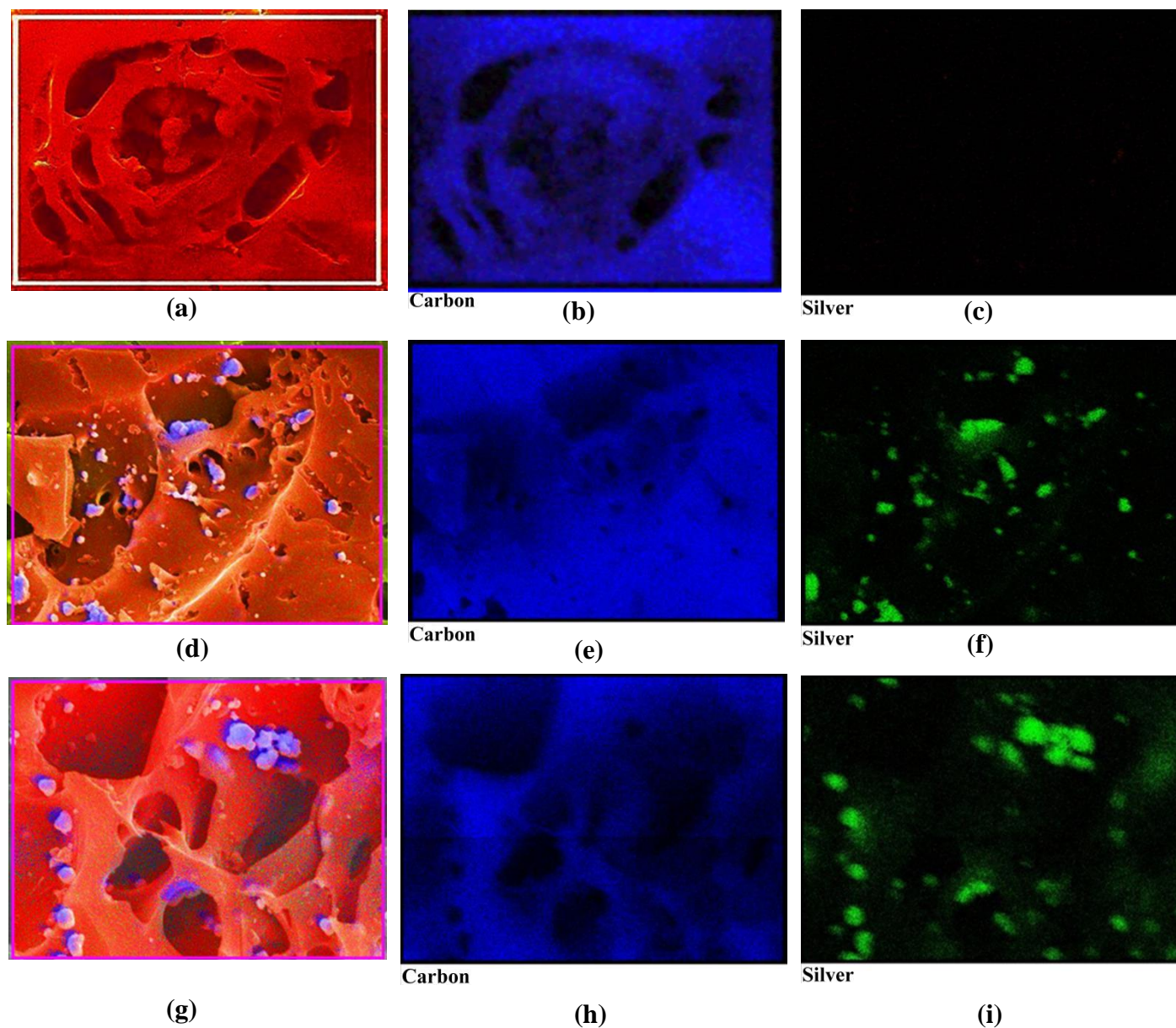
(g) Carbon **(h)** Silver **(i)**

Figure S8. FEG-SEM images on the area which is mapped for elemental mapping for (a) un-AC, (d) Ag-p-AC and (g) Ag-a-AC surface, respectively Elemental mapping of carbon [(b), (e) and (h)] and silver [(c), (f) and (i)] on AC, Ag-p-AC and Ag-a-AC surface, respectively.

Elemental mapping was performed for AC, Ag-p-AC and Ag-a-AC granules for identifying the location of attachment of Ag-NPs. Ag-p-AC and Ag-a-AC shows presence of Ag-NPs selectively on the external surface of the AC (Figure S8).

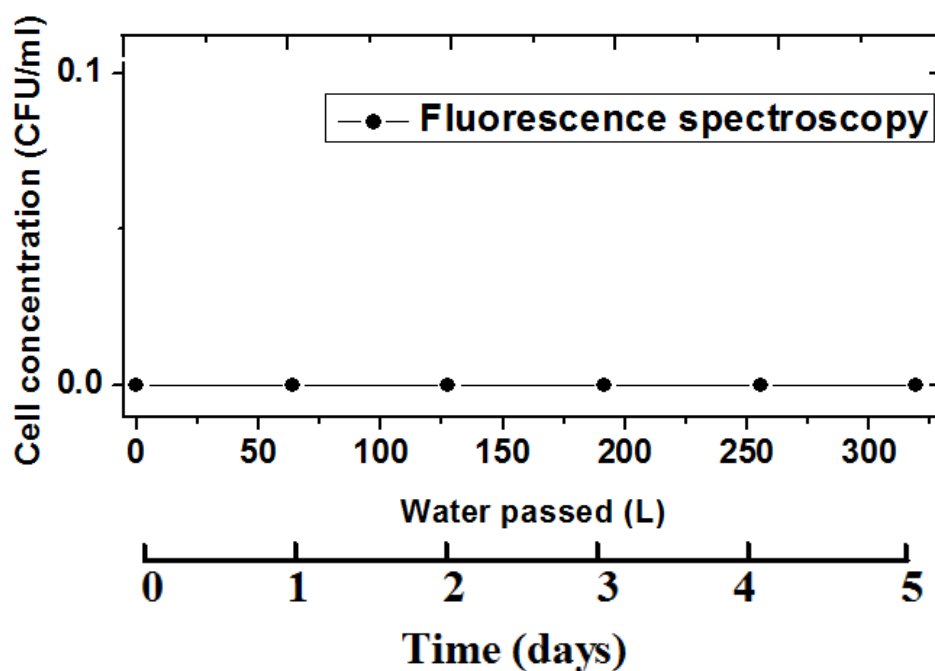**A.9 Quantification of cell concentration during long term cell-death experiments**

Figure S9. Long term performance assessment of the flow-column setup with Ag-a-AC packing, by measuring the cell concentration by fluorescence spectroscopy, for treating contaminated water having 10^4 CFU/ml *E. coli* cell in it at a flow rate of 2.66 L/h, treating 320 L of water over 5 days.

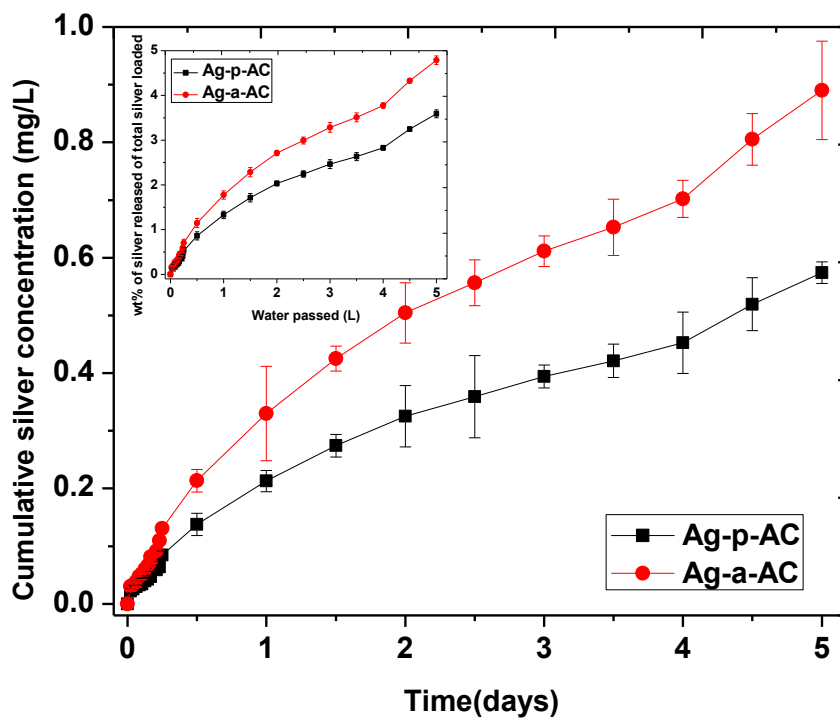**A.10 Quantification of Ag concentration during batch mode experiments**

Figure S10. Measurement of Ag concentration during batch mode experiment using 8 mg/ml of Ag-p-AC and Ag-a-AC hybrid. Inset shows the percentage of Ag released of total Ag during the batch experiment for both the hybrids.

A.11 Death rate constant fitting

The cell concentration vs. time plot from our batch mode cell-death experiment was shown in Figure S11. The experimental data fits well with an exponential decay curve of cell concentration [equation (A1)], with a death rate constant $k = 12.64$ h^{-1}, where, C_{bac0} *and* C_{bac} are the *E. coli* cell concentrations at t = 0 and any later value of t in CFU/ml.

$$C_{bac} = C_{bac_0} \exp(-kt)$$
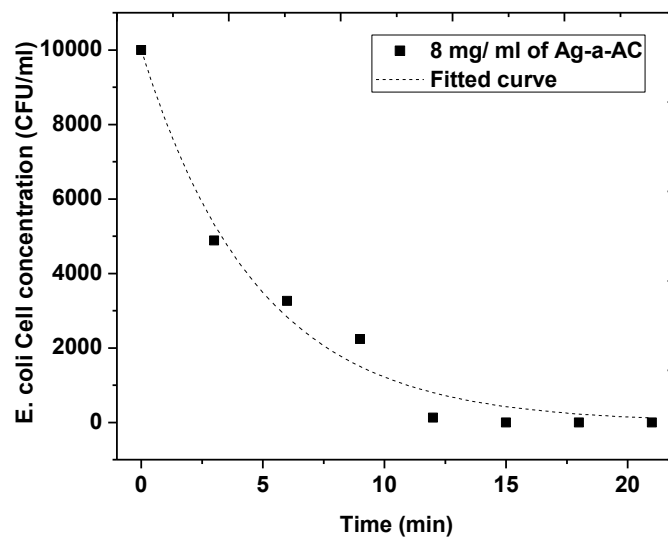
<div align="right">(A1)</div>

Figure S11. Death rate constant calculation from a fitted curve following Equation A1.

References

(1)   Biswas, P.; Bandyopadhyaya, R. Water Disinfection Using Silver Nanoparticle Impregnated Activated Carbon: E. Coli Cell-Killing in Batch and Continuous Packed Column Operation over a Long Duration. *Water Res.* **2016**, *100*, 105–115.